Proc. 15th Int. Symp. Origin of Matter and Evolution of Galaxies (OMEG15)
JPS Conf. Proc. **31**, 011009 (2020)
https://doi.org/10.7566/JPSCP.31.011009

Enrichment of Heavy Elements in Chemodynamical Evolution of Dwarf Galaxies

Yutaka Hirai[1], Shinya Wanajo[2,3,4] and Takayuki R. Saitoh[5,6]

[1]*RIKEN Center for Computational Science, 7-1-26 Minatojima-minami-machi, Chuo-ku, Kobe, Hyogo 650-0047, Japan*
[2]*Max-Planck-Institut für Gravitationsphysik (Albert-Einstein-Institut), Am Mühlenberg 1, D-14476 Potsdam-Golm, Germany*
[3]*RIKEN iTHEMS Research Group, 2-1 Hirosawa, Wako, Saitama 351-0198, Japan*
[4]*Department of Engineering and Applied Sciences, Faculty of Science and Technology, Sophia University, 7-1 Kioicho, Chiyoda-ku, Tokyo 102-8554, Japan*
[5]*Department of Planetology, Graduate School of Science, Kobe University, 1-1, Rokkodai-cho, Nada-ku, Kobe, Hyogo 657-8501, Japan*
[6]*Earth-Life Science Institute, Tokyo Institute of Technology, 2-12-1 Ookayama, Meguro-ku, Tokyo 152-8551, Japan*

E-mail: yutaka.hirai@riken.jp

(Received August 30, 2019)

Understanding of the enrichment history of heavy elements in galaxies is critical to clarify their astrophysical sites. Light trans-iron elements such as Sr, Y, and Zr show scatters of the ratio to Fe and Ba in metal-poor stars. However, the enrichment histories of these elements are not well understood. Here we report the enrichment of Sr in our high-resolution chemodynamical simulations of dwarf galaxies. We find that electron-capture supernovae (ECSNe) and rotating massive stars can contribute to the enrichment of Sr at low metallicity. We also find that ECSNe can produce stars enhanced in Sr to Ba ratio. The combinations of ECSNe, neutron star mergers, and hypernovae produce reasonable scatters of Sr to Zn ratios. Our results demonstrate that mass ranges of ECSNe greatly affect the Sr abundances at low metallicity.

KEYWORDS: galaxies: abundances, galaxies: dwarf, galaxies: evolution, methods: numerical, nucleosynthesis, stars: abundances

1. Introduction

Understanding the origin and enrichment history of heavy elements, i.e., pollution of elements in the interstellar medium by nucleosynthetic sources, is one of the open questions in nuclear astrophysics. Astronomical high-dispersion spectroscopic observations in the Local Group (LG) galaxies have shown that there are star-to-star scatters in the ratio of neutron-capture elements such as Sr, Ba, and Eu (e.g., [1]) for [Fe/H] $\lesssim -2.5$. Star-to-star scatters also exist in the ratio of different kinds of heavy elements such as Sr to Ba and Sr to Zn.

Nucleosynthetic studies have shown that neutron star mergers (NSMs) can be the astrophysical site of elements beyond the mass number of 110 (e.g., [2]). Observations of the afterglow of an NSM, GW170817 support that NSMs synthesize heavy elements (e.g., [3]). Recent studies of galactic chemical evolution, i.e., enrichment history of elements in galaxies also imply that they can produce Eu at low metallicity (e.g., [4–8]).

Astrophysical sites of light trans-iron elements such as Sr, Y, and Zr are not well understood. Scatters seen in the [Sr/Ba] ratios indicate that not all these elements are synthesized in the same site. Neutron-rich ejecta from electron-capture supernovae (ECSNe) or iron core-collapse supernovae

(CCSNe) in the low mass end are possible sites of these elements [9]. The weak-*s* process in rotating massive stars (RMSs) may also be a site of light trans-iron elements. However, the contribution of these sites on the galactic chemical evolution is not clear.

This study aims at clarifying the enrichment of heavy elements, mainly focusing on Sr in dwarf galaxies. Dwarf galaxies are the ideal object to study the impact of the uncertain astrophysical site because of their simple structures. We performed chemodynamical simulations of dwarf galaxies to study the enrichment of Sr self-consistently.

2. Method and Models

We performed a series of *N*-body/smoothed particle hydrodynamics (SPH) simulations of dwarf galaxies using ASURA [10, 11]. Gravity and hydrodynamics are computed with tree [12] and density-independent SPH [13] methods, respectively. Cooling and heating functions from 10 to 10^9 K are generated by CLOUDY [14]. In high density (> 100 cm^{-3}) and low-temperature region (< 1000 K), probabilistically selected gas particles are converted into star particles treated as a simple stellar population with the initial mass function of [15].

Feedback from star particles is implemented using the chemical evolution library (CELIB) [16]. Star particles exploded as supernovae distribute thermal energy of 10^{51} erg to surrounding gas particles. In this simulation, we assume that stars from 8 to 40 $M_\odot$ explode as CCSNe. Within the range of CCSNe, 5 % of stars from 20 to 40 $M_\odot$ and the low mass end are regarded as hypernovae (HNe) and ECSNe, respectively. The adopted mass range of ECSNe is shown in Table I. For yields of CCSNe and HNe, we adopt [17]. Yields of ECSNe are taken from [9]. In model C, we also assume the yields of RMSs for Sr and Ba [18]. For type Ia supernovae (SNeIa) and NSMs, we assume power law delay time distribution with the index of -1. The minimum delay times of SNeIa and NSMs are assumed to be 10^8 and 10^7 years, respectively. The yields are taken from [19] for SNeIa and [2] for NSMs. The assumed rate of NSMs corresponds to 0.2 % of stars with 8-20 $M_\odot$. We also assume that stars with 1 to 6 $M_\odot$ distribute elements as asymptotic giant branch (AGB) [20]. Distributed elements are diffused to surrounding gas particles following the turbulence motivated metal diffusion model [21].

Table I. List of models. From left to right, columns show the name of models, adopted mass ranges of ECSNe at [Fe/H] = -3, with (yes) or without (no) assumption of RMSs. Models A and C adopt the metallicity-dependent mass range of ECSNe predicted by the stellar evolution calculation [22]. Model B assumes the constant mass range of ECSNe for metallciity (Z) $> 10^{-5}$.

Model	ECSNe	RMSs
A	8.2–8.4 $M_\odot$	no
B	8.2–9.2 $M_\odot$	no
C	8.2–8.4 $M_\odot$	yes

We adopt an isolated dwarf galaxy model as an initial condition [23,24]. Dark matter and gas particles are distributed following the pseudo-isothermal profile. The total mass of the halo is $7\times10^8 M_\odot$. The total number of particles and gravitational softening length are 2.6×10^5 and 7.8 pc, respectively. The total stellar mass and mean metallicity are 3.2×10^6 $M_\odot$ and -1.45 at 13.8 Gyr from the beginning of the simulation, respectively.

3. Results and Discussion

Enrichment of Sr is affected by ECSNe, NSMs, RMSs, and AGB stars. Figure 1 shows [Sr/Fe] as a function of [Fe/H] in models A (panel a), B (panel b), and C (panel c). In these models, the first NSM occurs at [Fe/H] ≈ -3. This result means that ECSNe or RMSs mainly contribute to the enrichment of Sr for the lowest metallicity. Model A shows depleted [Sr/Fe] (≈ -1.5) ratio. Even if

the ejecta from ECSN are enhanced in Sr, such ejecta are soon diluted because of the low rate of ECSNe. For [Fe/H] > -3, both NSMs and ECSNe contribute to the enrichment of Sr. The effect of AGB stars can only be seen for [Fe/H] ≈ -1 owing to the strong dependence on the yields.

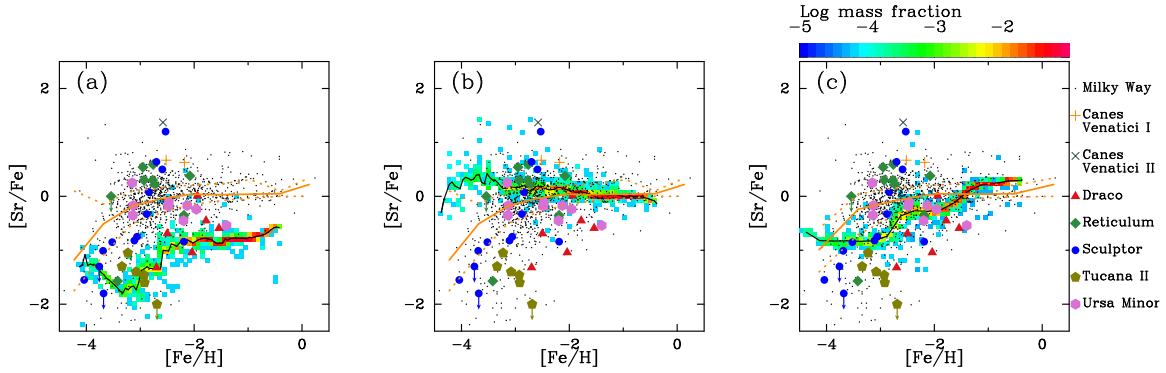

Fig. 1. [Sr/Fe] as a function of [Fe/H] in models A (panel a), B (panel b), and C (panel c). Color coding from blue to red shows the mass fraction of computed stars from 10^{-5} to 10^{-1}. Black solid curves represent the median of these values. Plots denote observed abundances in the LG galaxies (SAGA database [25, 26]). Names of galaxies for each kind of symbols are shown in the legend. Orange solid and dashed curves represent median, first, and third quartiles of the Sr abundances in the Milky Way, respectively.

Mass ranges of ECSNe affect the enrichment of Sr. Model B adopts the wider mass range of ECSNe than that of model A (Table I). This model shows [Sr/Fe] ~ 0 for whole metallicity range (Fig. 1b). RMSs also increase the [Sr/Fe] ratios. Model C adopts RMSs in addition to ECSNe. As shown in Fig. 1c, [Sr/Fe] ratios in model C are higher than those in model A. These results suggest that mass ranges of ECSNe and the contribution of RMSs affect the abundance of Sr. To explain the median value of [Sr/Fe] ratios in the Milky Way, wider mass ranges of ECSNe than those predicted by [22] or contribution of RMSs are necessary. However, mass ranges of ECSNe are still highly uncertain. The prediction of their mass ranges from stellar evolution calculations largely depends on parameters such as mass loss rate, overshooting, and the efficiency of third dredge-up [22]. The yields of Sr from RMSs also greatly depend on the rotational speed of stars. Accurate determination of mass ranges of ECSNe and rotational velocity of stars is required to constrain the enrichment of Sr more precisely.

The effect of ECSNe is seen in [Sr/Ba] ratios. Figure 2a shows [Sr/Ba] as a function of [Fe/H] in model A. For [Fe/H] < -3, most stars are enhanced in [Sr/Ba]. Wanajo et al. [9] have shown that ECSNe synthesize a large amount of Sr but do not produce Ba. Because of this property of nucleosynthesis in ECSNe, stars formed from the ejecta from ECSNe have enhanced [Sr/Ba] ratios. For [Fe/H] < -3, Ba comes from the *s*-process in AGB stars. Because of the slow chemical evolution in our models, AGB stars can contribute to the enrichment even at [Fe/H] ~ -4. However, the abundance of Ba from AGB stars is too low ([Ba/H] < -6) to detect in the observations. After the first NSM occurs, the [Sr/Ba] ratio decreases to [Sr/Ba] ≈ 0. The variations of the yields of NSMs or binary black-hole neutron star mergers and weak *s*-process in RMSs can make lower [Sr/Ba] ratios.

Figure 2b shows [Sr/Zn] as a function of [Fe/H] in model A. In this model, Zn is mainly synthesized by ECSNe and HNe. As shown in this figure, the computed [Sr/Zn] ratio is roughly overlapped with observations. This result implies that the combinations of ECSNe, HNe, and NSMs can cause variations of [Sr/Zn] ratios.

In this study, we have adopted ECSNe, NSMs, RMSs, and AGB stars as nucleosynthetic sites of Sr. For [Fe/H] $\lesssim -3$, ECSNe or RMSs mainly produce Sr. NSMs begin to contribute to Sr for [Fe/H] $\gtrsim -3$ in our models. Contribution of AGB stars on the abundances of Sr can be seen for [Fe/H] $\gtrsim -1$. In the LG dwarf galaxies, there are variations of the abundances of Sr. We find that timing of NSMs can cause variations of Sr abundances. In dwarf galaxies, the effect of one NSM can affect the

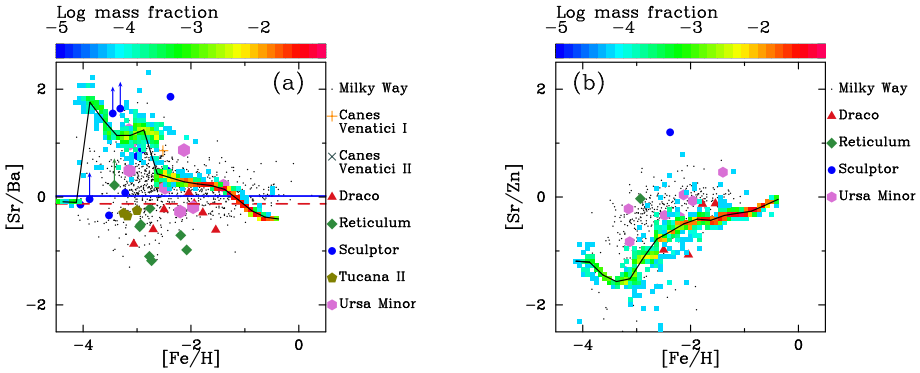

Fig. 2. Same as Fig. 1, but for [Sr/Ba] (panel a) and [Sr/Zn] (panel b) in model A. Blue-solid and red dashed lines in panel a represent the [Sr/Ba] ratios of solar *s*- and *r*-processes, respectively [27].

abundances of Sr. On the other hand, the Milky Way has more extensive scatters of [Sr/Fe] ratios than those of our models. These large scatters can be caused by the accretion of different mass galaxies [7]. Future high-resolution cosmological zoom-in simulations will make it possible to compare with observed heavy element abundances directly.

This work was supported by JSPS KAKENHI Grant Numbers 19K21057 and 19H01933. YH is supported by the SPDR program at RIKEN. Numerical computations and analysis were carried out on Cray XC40, XC50, and computers at YITP and CfCA/NAOJ. This research has made use of NASA's Astrophysics Data System.

References

[1] C. M. Sakari, V. M. Placco, E. M. Farrell *et al.*, Astrophys. J. **868**, 11 (2018).
[2] S. Wanajo, Y. Sakiguchi, N. Nishimura *et al.*, Astrophys. J. **789**, L39 (2014).
[3] M. Tanaka, Y. Utsumi, P. A. Mazzali *et al.*, Publ. Astron. Soc. Jpn. **69**, 102 (2017).
[4] Y. Ishimaru, S. Wanajo, and N. Prantzos, Astrophys. J. **804**, L35 (2015).
[5] Y. Hirai, Y. Ishimaru, T. R. Saitoh *et al.*, Astrophys. J. **814**, 41 (2015).
[6] Y. Hirai, Y. Ishimaru, T. R. Saitoh *et al.*, Mon. Not. R. Astron. Soc. **466**, 2474 (2017).
[7] T. Ojima, Y. Ishimaru, S. Wanajo, N. Prantzos, and P. François, Astrophys. J. **865**, 87 (2018).
[8] C. J. Haynes and C. Kobayashi, Mon. Not. R. Astron. Soc. **483**, 5123 (2019).
[9] S. Wanajo, B. Müller, H.-T. Janka, and A. Heger, Astrophys. J. **852**, 40 (2018).
[10] T. R. Saitoh, H. Daisaka, E. Kokubo *et al.*, Publ. Astron. Soc. Jpn. **60**, 667 (2008).
[11] T. R. Saitoh, H. Daisaka, E. Kokubo *et al.*, Publ. Astron. Soc. Jpn. **61**, 481 (2009).
[12] J. Barnes and P. Hut, Nature **324**, 446 (1986).
[13] T. R. Saitoh and J. Makino, Astrophys. J. **768**, 44 (2013).
[14] J. Ferland, R. L. Porter, P. A. M. van Hoof *et al.*, Rev. Mex. Astron. Astrofs **49**, 1 (2013).
[15] P. Kroupa, Mon. Not. R. Astron. Soc. **322**, 231 (2001).
[16] T. R. Saitoh, Astron. J. **153**, 85 (2017).
[17] K. Nomoto, C. Kobayashi, and N. Tominaga, Annu. Rev. Astron. Astrophys **51**, 457 (2013).
[18] M. Limongi and A. Chieffi, Astrophys. J. **237**, 13 (2018).
[19] I. R. Seitenzahl, F. Ciaraldi-Schoolmann, F. K. Röpke *et al.*, Mon. Not. R. Astron. Soc. **429**, 1156 (2013).
[20] S. Cristallo, O. Straniero, L. Piersanti, and D. Gobrecht, Astrophys. J., Suppl. Ser. **219**, 40 (2015).
[21] Y. Hirai and T. R. Saitoh, Astrophys. J. **838**, L23 (2017).
[22] C. L. Doherty, P. Gil-Pons, L. Siess, J. C. Lattanzio, and H. H. B. Lau, Mon. Not. R. Astron. Soc. **446**, 2599 (2015).
[23] Y. Hirai, T. R. Saitoh, Y. Ishimaru, and S. Wanajo, Astrophys. J. **855**, 63 (2018).
[24] Y. Hirai, S. Wanajo and T. R. Saitoh, Astrophys. J. **885**, 33 (2019).
[25] T. Suda, Y. Katsuta, S. Yamada *et al.*, Publ. Astron. Soc. Jpn. **60**,1159 (2008).
[26] T. Suda, J. Hidaka, W. Aoki *et al.*, Publ. Astron. Soc. Jpn. **69**, 76 (2017).
[27] J. Simmerer, C. Sneden, J. J. Cowan *et al.* Astrophys. J. **617**, 109 (2004).